3D-printed dielectric helical THz Waveguides

Dominik Vogt* and Rainer Leonhardt*
*Dodd-Walls Centre for Photonic and Quantum Technologies,
and Department of Physics, The University of Auckland,Private Bag 92019, Auckland 1142, New Zealand

***Abstract*—We report on a 3D-printed helical waveguide to increase the bandwidth of a low-loss dielectric tube Terahertz (THz) waveguide. The helical design prevents the multiple reflections in the tube cladding hence avoiding the pronounced interference pattern in the attenuation spectrum of a dielectric tube waveguide. Both THz time-domain spectroscopy (THz-TDS) measurements and finite-difference time-domain (FDTD) simulations consistently confirm the extended bandwidth of the dielectric helical waveguide. In addition, numerical investigations reveal that the broadband behavior of the 3D-printed helical waveguide is not critical with respect to the absorption of the waveguide material.**

I. Introduction

The dielectric tube THz waveguide is well known and has drawn interest particularly due to its simplicity and appealing guidance properties for THz radiation [1]. The guidance of the tube is based on the Fabry-Perot effect of the cladding. Consequently, the attenuation spectrum of the dielectric tube shows pronounced interference patterns, limiting the bandwidth of the waveguide. The 3D-printed helical waveguide presented in this work is a simple approach to effectively extend the bandwidth of a dielectric tube THz waveguide. Moreover, the helical design fabricated in this work provides a superior flexibility in comparison to the rigid dielectric tube waveguides.

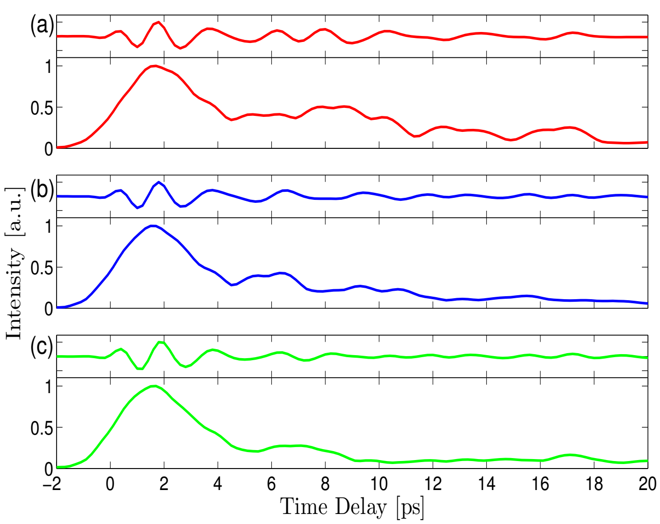

Fig. 1. Experimentally obtained time-dependent E-fields (top) and the corresponding intensity profiles (bottom) of a) a dielectric tube waveguide and helical waveguides with a pitch of b) 0.9 mm and c) 1.2 mm.

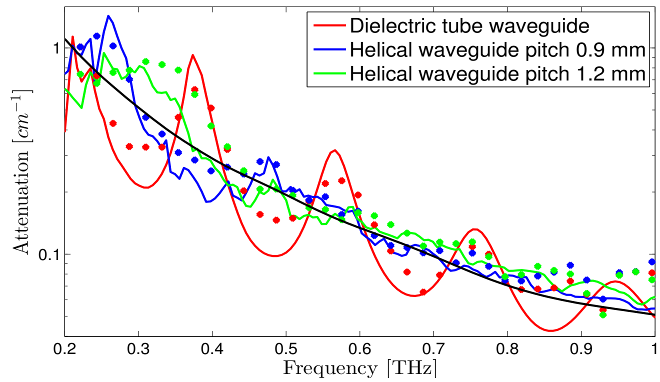

Fig. 2. Measured (dots) and simulated (solid) attenuation curves in logarithmic scale for a dielectric tube (red, a) in Fig. 1) and helical waveguides with a pitch of 0.9 mm (blue, b) in Fig. 1) and 1.2 mm (green, c) in Fig. 1). The continuous black line shows the attenuation of a dielectric tube waveguide with an infinite cladding thickness.

II. Results

The dielectric helical waveguides are fabricated with a commercially available Project 3500HD Plus 3D printer with specifications of X-Y resolution of 375 DPI (equivalent to 68 μm linewidth) and 790 DPI in Z-resolution (equivalent to 32 μm linewidth) [2]. The deployed UV curable polymer is commercially known as VisiJet® M3. The helical waveguides investigated in this work are designed with an inner diameter of 4 mm. The pitches of the helices were chosen to be 0.9 mm and 1.2 mm, while the cladding strand has a square cross section of 0.6 mm by 0.6 mm. We compare our helical waveguides with a standard tube with an inner diameter of 4 mm and a cladding thickness of 0.6 mm. The waveguides are experimentally characterized in the frequency range from 0.2 − 1.0 THz with a THz-TDS setup. Specially designed symmetric-pass lenses with a focal length of 100 mm and NA = 0.25 couple the free-space THz pulse into the waveguides citelens.

Fig. 1 shows the normalized intensity profiles calculated from the measured temporal profiles of the tube and the two helical waveguides. The measured and corresponding simulated attenuation curves are shown in Fig. 2. Our simulations are performed with a freely available FDTD software package [4] and take the experimentally determined dielectric properties of the material into account. The obtained numerical and experimental results show an excellent agreement and confirm that the helical design substantially reduces the amplitude of the afterpulses (see Fig. 1), or equivalently the modulation in the loss spectrum (see Fig. 2) of the tube caused by the Fabry-Perot effect. For ease of comparison and to guide the eye, the attenuation curve of a Fabry-Perot effect free dielectric tube waveguide with an infinite cladding is shown in Fig. 2 (continuous black curve).

Please note that while the material loss has to be considered in the simulations in order to match the modulation strength and waveguide loss measured for the dielectric tube waveguide, the absorption of the waveguide material is not essential for the desired broadband behavior of the helical waveguide. To emphasize the latter, we repeat the previously performed simulations but neglect the imaginary part of the dielectric function of the waveguide material. Moreover, for the sake of simplicity, we perform the simulations with a dispersion free material and use the measured material refractive index at 0.6 THz. The obtained confinement loss curves including the curve of an infinite cladding dielectric tube waveguide are shown in Fig. 3. Comparing Fig. 2 and Fig. 3, it is obvious that the absorption of the waveguide material does not significantly improve the broadband behavior of the 3D printed dielectric helical waveguide, and that it primarily depends on the pitch of the helical waveguide.

The normalized electric field energy density distribution guided in the dielectric tube and both helical waveguides are shown in Fig. 4 a) and b),c), respectively. The energy densities are depicted in the vicinity of the cladding of the waveguides at the same instant on a logarithmic scale. The semi-transparent overlay of the corresponding dielectric structure in Fig. 4 eases the interpretation of the shown energy distributions. Fig. 4 a) clearly reveals the pronounced fields reflected forth and back inside the tube cladding causing the strong afterpulses inside the dielectric tube waveguide. In contrary, the helical design prevents the reflection of the evanescent fields back into the waveguide center, and therefore the formation of afterpulses. This effect is nicely visualized in Fig. 4 b) and c), and also demonstrates its dependence on the pitch of the dielectric helical waveguide. However, since this work shows a proof of concept no further optimization of the performance of the helical design has been conducted.

III. Conclusion

We demonstrated that the proposed 3D-printed helical waveguide diminishes the impact of the Fabry-Perot effect in a dielectric tube waveguide. The experimentally and numerically obtained attenuation curves verify that our helical design exhibits low-loss guidance, with superior bandwidth compared to a standard dielectric tube. Furthermore, numerical investigations presented in this work reveal that the fabrication of the dielectric helical waveguide is not restricted to a limited range of materials suitable for the THz frequency range. The simulated electric field energy density distributions clearly demonstrate the strong restriction of the multiple reflections in the cladding strand of a 3D printed dielectric waveguide in comparison to a standard dielectric tube. Further investigations will be focused both on design optimization and measurements of curved sections of these waveguides.

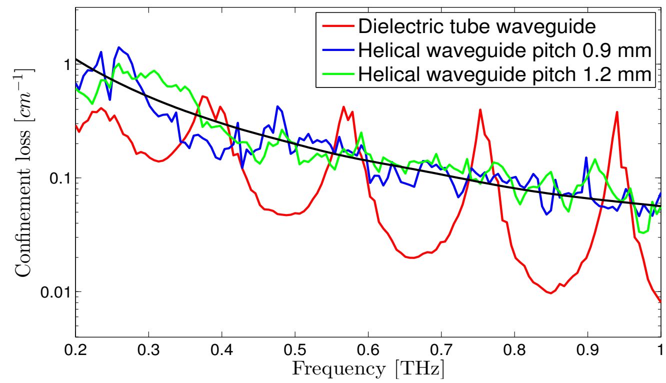

Fig. 3. Simulated confinement loss curves on a logarithmic scale for a dielectric tube (red) and helical waveguides with a pitch of 0.9 mm (blue) and 1.2 mm (green). The material absorption, i.e. the imaginary part of the dielectric function of the waveguide material, is omitted. Furthermore, a frequency independent material refractive index of about 1.65 was used in the simulations. The continuous black line shows the attenuation of a dielectric tube waveguide with a infinite cladding thickness.

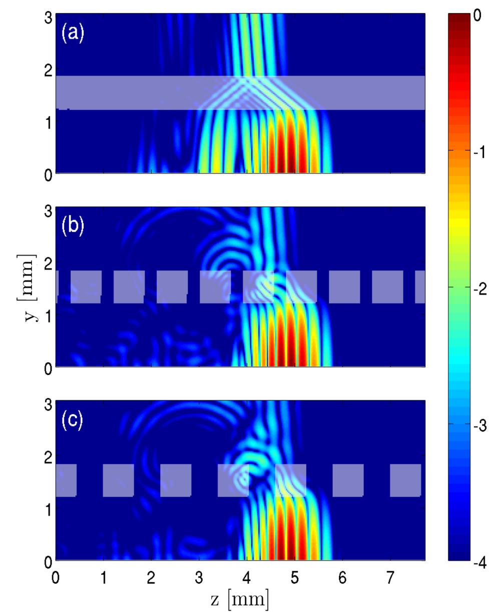

Fig. 4. Normalized spatial distribution of the simulated electric field energy density in the vicinity of the cladding of a) a dielectric tube waveguide and helical waveguides with a pitch of b) 0.9 mm and c) 1.2 mm in logarithmic scale. The THz-pulse is propagating in positive z-direction and is depicted in all sub-figures at the same time delay. An overlay of the corresponding lossy dielectric material is shown for each waveguide design. The origin is arbitrarily defined at the lower left corner of each sub-figure.

References

[1] Hualong Bao, Kristian Nielsen, Ole Bang and Peter Uhd Jepsen, “Dielectric tube waveguides with absorptive cladding for broadband, low-dispersion and low loss THz guiding”, Sci. Rep. 5:7620, 2015.

[2] http://www.3dsystems.com

[3] Y. H. Lo and R. Leonhardt, “Aspheric Lenses for Terahertz Imaging“, Opt. Express, vol. 16, pp. 15991-15998, 2008.

[4] Ardavan F. Oskooi, David Roundy, Mihai Ibanescu, Peter Bermel, J. D. Joannopoulos, and Steven G. Johnson, “MEEP: A flexible free-software package for electromagnetic simulations by the FDTD method“, Computer Physics Communications, vol. 181, pp. 687-702, 2010.